Cross-Domain Document Object Detection: Benchmark Suite and Method

Kai Li[1], Curtis Wigington[2], Chris Tensmeyer[2], Handong Zhao[2],
Nikolaos Barmpalios[3], Vlad I. Morariu[2], Varun Manjunatha[2], Tong Sun[2], Yun Fu[1]
[1]Northeastern University, [2]Adobe Research, [3]Adobe Document Cloud

{kaili,yunfu}@ece.neu.edu
{wigingto,tensmeye,hazhao,barmpali,morariu,vmanjuna,tsun}@adobe.com

Abstract

Decomposing images of document pages into high-level semantic regions (e.g., figures, tables, paragraphs), document object detection (DOD) is fundamental for downstream tasks like intelligent document editing and understanding. DOD remains a challenging problem as document objects vary significantly in layout, size, aspect ratio, texture, etc. An additional challenge arises in practice because large labeled training datasets are only available for domains that differ from the target domain. We investigate cross-domain DOD, where the goal is to learn a detector for the target domain using labeled data from the source domain and only unlabeled data from the target domain. Documents from the two domains may vary significantly in layout, language, and genre. We establish a benchmark suite consisting of different types of PDF document datasets that can be utilized for cross-domain DOD model training and evaluation. For each dataset, we provide the page images, bounding box annotations, PDF files, and the rendering layers extracted from the PDF files. Moreover, we propose a novel cross-domain DOD model which builds upon the standard detection model and addresses domain shifts by incorporating three novel alignment modules: Feature Pyramid Alignment (FPA) module, Region Alignment (RA) module and Rendering Layer alignment (RLA) module. Extensive experiments on the benchmark suite substantiate the efficacy of the three proposed modules and the proposed method significantly outperforms the baseline methods. The project page is at https://github.com/kailigo/cddod.

1. Introduction

Document Object Detection (DOD) is the task of automatically decomposing a document page image into its structural and logical units (e.g., figures, tables, paragraphs). DOD is critical for a variety of document image analysis applications, such as document editing, document structure analysis and content understanding [31, 1, 30]. Two popular document formats, image (e.g. scanned and camera-captured documents) and PDF, do not explicitly encode document structure: images consist of pixels, while PDFs consist of vector, raster, and text marking operations that allow a document to be faithfully reproduced across devices (e.g., printers, and displays).

Though recent advances in object detection for natural scene images are impressive [27, 21], directly applying the same model to document images is likely sub-optimal due to large domain differences. For example, document objects are more diverse in aspect ratio and scale than natural scene objects: tables may occupy a whole page, page numbers can be as small as a single digit, and a single line of text spanning the page has an extreme aspect ratio. The intra-class variance of document objects is also usually larger than that of natural scene objects. Text can have arbitrary font face, style, position, orientation, and size. Table cells can be filled with arbitrary content as long as they are aligned in a grid layout. Document layouts and objects are also modular entities, so that, for example, examining the left half of a paragraph gives little information on how wide that paragraph is. In contrast, missing parts of natural objects and scenes can be reasonably in-painted based on surrounding context [26].

Another key challenge is that many factors influence the appearance of a document, such as document type (e.g. menu, scientific article), layout (e.g. Portrait vs Landscape or single/multi-column), and written language. While learning a single model that can handle all varieties of documents is desirable, constructing such a comprehensive dataset appears infeasible. Because labeled data is not available for every kind of document collection, we are motivated to examine cross-domain DOD. In cross-domain DOD, we leverage labeled data in the source domain and unlabeled data in the target domain to train a detector for the target domain.

To facilitate advancements in this field, we establish a benchmark suite on which cross-domain DOD models can be trained and evaluated. The benchmark suite consists of different types of document datasets; each serves as one do-

main. Each dataset is composed of the following components. (1) Document page images and bounding box annotations. These are essential data for detection model training and evaluation. (2) Raw PDF files used to generate the page images. The raw PDF files preserve the information lost when converting PDF pages to images, like the text and some meta-data. These extra sources of information may complement the visual information and benefit the detection task. (3) PDF rendering layers. A PDF page is in fact a mixture of text, vector, and raster content. These three content types can be rendered into separate layers for a PDF page, with each layer containing the pixel rendering arising only from one content type (text, vector, or raster). These rendering layers provide a structural abstraction of the PDF page and thus could be helpful for the detection task as well.

In addition to the benchmark suite, we propose a novel cross-domain DOD model, which builds on top of the Feature Pyramid Networks (FPN) object detector [21] and addresses the domain shift problem by introducing three novel modules. The first module is the Feature Pyramid Alignment (FPA) module. FPA performs dense pixel-wise alignment between feature pyramids from source and target domains. Since each layer of the pyramids mixes both high- and low-level features, explicitly pushing cross-domain feature pyramid layers closer to each other achieves joint alignment of both low- and high-level semantics. The second module is the Region Alignment (RA) module. RA aims to enhance the alignment of semantically meaningful foreground regions from the two domains and explicitly pushes regions extracted from the two domains closer to each other. We adopt the focal loss [22] into our objective function to focus more on hard-to-align samples. The last module is the Rendering Layer Alignment (RLA) module. We utilize the PDF rendering layers available in our benchmark suite and generate for each page a mask which specifies the rendering layer that each pixel belongs to. RLA takes the mask as a kind of segmentation map for the page and trains an auxiliary segmentation task to further align the domains by predicting the masks from images of the two domains.

The contribution of this paper is three-fold:

- We establish a benchmark suite for cross-domain DOD model training and evaluation. To our best knowledge, we are the first to study this problem and the benchmark is the first one in this area.

- We propose a novel cross-domain DOD model which introduces three novel modules to approach the domain shift problem. The three modules complement with each other and align the domains from both general image perspective and specific document image perspective.

- Our model effectively mitigates the domain shift problem and significantly advances the baseline performance on the benchmark suite.

2. Related Work

Our work is related to document object detection and cross-domain object detection for natural scene images.

2.1. Document Object Detection

Most existing approaches to document object detection focus on certain types of objects, e.g., tables, figures, or mathematical formulas. Early works rely on various heuristic rules to extract and identify these objects from document images [24, 9, 32]. These approaches often involve a set of hyper-parameters, which are difficult to adapt to new document domains. Recent works are usually data-driven and approach the problem with machine learning techniques, or a hybrid of heuristic rules and learning models. Taking advantage of the impressive progress of object detection on natural scene images, many works adapt natural image object detectors by considering the uniqueness of the document images [30, 11]. He et al. [13] propose a two-stage approach to detect tables and figures. In the first stage, the class label for each pixel is predicted using a multi-scale, multi-task fully convolutional neural network. Then in the second stage, heuristic rules are applied on the pixel-wise class predictions to get the object boxes. Gao et al. [8] utilize meta-data information of PDF files and detect formulas using a model that combines CNN and RNN. A few works detect multiple types of document objects jointly in a single framework [7]. Yi et al. [34] adapt the region proposal approach and redesign the CNN architecture of common object detectors by considering the uniqueness of document objects. [20] first performs deep structure prediction and gets the primitive region proposals from each column region. Then, the primitive proposals are clustered and those within the same cluster are merged as a single object instance.

2.2. Cross-Domain Object Detection

Existing cross-domain object detection methods can be roughly divided into two categories: ones that are based on feature alignment and ones that are based on self-training. Methods in the former category train models from which domain-agnostic feature representations can be obtained for images from both domains [37, 29, 3, 15]. To achieve this, these methods usually train domain classifiers and feature extraction models in an adversarial manner until the domain classifiers cannot distinguish the domains of the images from which the features are extracted. The difference lies in the position and way that the domain classifiers are used. Methods in the latter category train the models recursively by generating pseudo bounding box labels for target images and updating the models with the generated pseudo labels [18, 16, 17, 28]. Different methods vary in how they generate the pseudo labels or update the model. Both categories of methods benefit from style transfer techniques
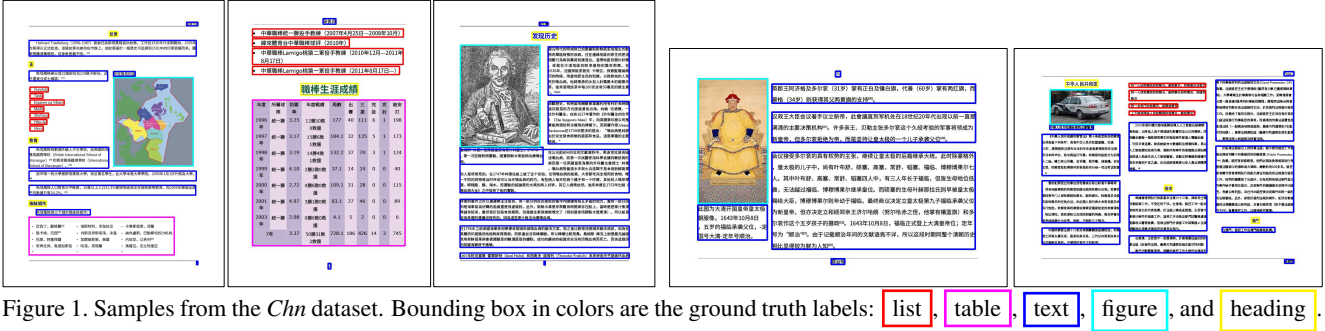
Figure 1. Samples from the *Chn* dataset. Bounding box in colors are the ground truth labels: list , table , text , figure , and heading .

which first train a style transfer model (e.g., CycleGAN [36]) using images from both domains and then apply the model to translate images from the source domain as the style of the target domain. Using this approach, labeled images of a similar style as that of the target domain can be obtained, which facilitates further domain alignment [16, 19].

Our cross-domain DOD model inherits the merits of the recent cross-domain object detectors for natural scene images. We follow the line of approaches which addresses domain shifts by explicitly performing feature alignment. But instead of aligning either low-level features [29] or high-level features [3, 37], or alignment them both separately [15], we align them jointly with the feature pyramids, as each layer of which is a mixture of both low and high-level features. Further, we propose a focal loss based region proposal alignment module which aims to enhance the alignment of foreground regions. This module is different from the previous methods [3, 15] that treat all region proposal equally, and instead focuses more on the hard-to-align proposals. Moreover, we utilize the rendering layer data available for the document datasets and generate from them segmentation masks for both source and target images. We use the masks as additional cues to align the domains by training an auxiliary segmentation task.

3. Benchmark Suite

There are a few existing datasets for document object detection. However, these datasets usually include annotations only for certain types of objects, e.g., table [12, 5] or mathematical formulas [23]. [7] established a dataset which contains annotations for three types of objects: table, figure and mathematical formula. However, this dataset is no longer publicly available. In addition, the largest existing dataset contains only 2000 page images [7], which is too small for modern deep object detectors.

Very recently, [35] released a large-scale dataset for document object detection. It contains annotations for more than 3.5 million object instances from over 360 thousand page images extracted from medical journal articles. The annotated objects cover 5 classes: text, title, list, table and figure. The annotations are obtained automatically by

matching the XML representations created by the publisher and the PDF content. We take advantage of this dataset and randomly select a subset, referred to as *PubMed* in this work, for our cross-domain experiments. *PubMed* includes 12871 images and 257830 bounding box annotations. We randomly split the dataset into 9653 images for training and 3218 images for testing. Note that the definition of the "list" class in [35] is a single region that contains all the numbered or bulleted items. This definition is not consistent with that of the other datasets within the benchmark suite. We therefore preprocess the annotations of "list" in [35] and split the ground truth bounding boxes into small ones for every individual items by detecting the list bullets or numbers.

Another dataset included in the benchmark suite is *Chn*, a synthesized Chinese document dataset. It is generated by a tool which crawls Chinese Wikipedia pages and converts the content into natural looking well-tagged (bounding box annotations can be obtained from the tags) PDF files. Specifically, the tool converts each Wikipedia HTML page into a document by (a) randomly defining a layout to arrange the HTML content in document pages and (b) selecting the style of that content. The layout generation is controlled by a set of layout parameters that define the overall appearance and includes margins, number of columns, the white-space between the columns and the presence of headers / footers. Content is arranged based on the defined layout, which results in a Document Object Model (DOM) where most of the DOM elements correspond to tags generated in the final PDF. The styling parameters, which define the look and feel of paragraphs, headers etc., include font (family, size and style), as well as coloring schemes for lines (e.g., for tables). It should be noted that styling parameters follow a hierarchical pattern; for example defining the size of the base font automatically sets the font size for all the headers (h1, h2, etc.). Finally, to enforce the generated documents to be as natural looking as possible, the layout and styling parameters are randomly sampled from a distribution computed using real world document statistics.

After filtering out low quality samples, we obtain 8005 page images, with 203456 bounding box annotations for the same 5 classes as that of *PubMed*. We further randomly select 5000 and 3005 page images for training and test, re-
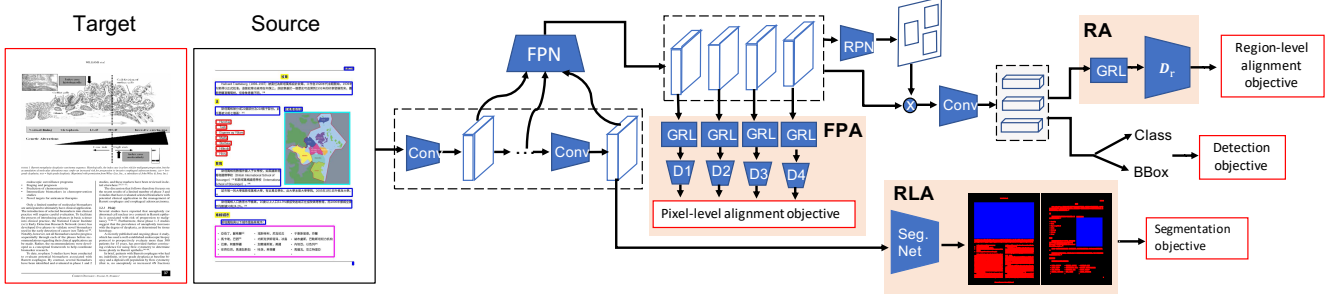
Figure 2. Summary of the proposed method. We build on FPN [21] and introduce three novel modules (masked in light pink) to align different document domains (English and Chinese in this example). The Feature Pyramid Alignment (FPA) module includes four binary domain classifiers $\{D_1, D_2, D_3, D_4\}$, corresponding to the four feature layers of the pyramid. Each of these D_j classifies pixels by image domain. The Region Alignment (RA) module is a binary domain classifier D_i, serving to classify the region proposals. The Rendering Layer Alignment (RLA) module is a segmentation network, which predicts rendering layer masks from the FPN layer. All binary domain classifiers follow a Gradient Reverse Layer (GRL) [6], which reverses the loss gradient during training and helps realize min-max optimization in each back-propagation.

spectively. Figure 1 shows some samples from the dataset.

For the two datasets above, besides the images and the corresponding bounding box annotations, we also provide the raw PDF files used to generate the page images. Most meta-data are lost when converting PDF pages to images. We thus provide the source PDF files in our benchmark suite to enable future research to take advantage of these meta-data and advance the detection task or other relevant tasks, as Yang et. al. [33] did. They showed that the textual information in PDF files are helpful for document semantic structure extraction, when properly combined with the visual images. We also believe the textual information can also benefit the detection task for multi-modal (visual + textual) methods.

Moreover, we also provide the PDF rendering layers associated with the PDF pages. A PDF page is in fact rendered by a mixture of textual drawings, vector drawings, and raster drawings. Drawings of the same type lie in the same rendering layer, and we can extract the layers from PDF files. These rendering layers provide structural abstraction of PDF pages and thus shall be helpful for the detection task as well.

We also utilize a human-annotated dataset for performance evaluation. The dataset includes 19355 page images and 257830 bounding box annotations for legal reports. We randomly select 9684 images for training and the remaining 9671 for testing. This dataset is annotated with the same 5 classes as the other two datasets and we also utilize the rendering layers in this work. We will refer this dataset as *legal* in future use.

4. Method

Figure 2 illustrates our proposed method. It is based on the Feature Pyramid Networks (FPN) and includes three novel domain alignment modules, namely, the Feature Pyramid Alignment (FPA) module, the Region Alignment (RA)

module and the Rendering Layer Alignment (RLA) module.

4.1. Feature Pyramid Networks

FPN exploits the pyramidal feature hierarchy of convolutional neural networks and builds a feature pyramid of high-level semantics for all the layers. It is independent of the backbone convolutional architecture (we adopt the standard ResNet-101 [14] as the backbone). With the feature hierarchy $\{C_1, C_2, C_3, C_4\}$ from the layer1, layer2, layer3, and layer4 outputs of ResNet-101, FPN iterates from the coarsest feature map, up-samples it by a factor of 2 for the spatial resolution, and merges it (by element-wise addition) with the preceding map, which has undergone a 1×1 convolution to reduce channel dimensions. The merged feature map is then smoothed by a 3×3 convolution to produce the final feature map. This iteration process outputs a feature pyramid $\{P_1, P_2, P_3, P_4\}$, where

$$P_i = conv3(up\_sample(P_{i+1})+conv1(C_i)), \ i = 1, 2, 3, 4, \tag{1}$$

where $conv1$, $conv3$, and up_sample are 1×1, 3×3 and up-sampling operations, respectively. Note that P_5 is the result of 1×1 convolution on C_4, i.e., $P_5 = conv1(C_4)$.

Region proposals are extracted from all feature pyramid layers $\{P_1, P_2, P_3, P_4\}$ by the region proposal network (RPN). The obtained region proposals are then forwarded to the feature extraction module to obtain a feature vector for each proposal. For an image from the source dataset, we calculate the detection loss using the bounding box ground truth:

$$L_{det}^s = L_{reg}(x^s, y^s) + L_{cls}(x^s, y^s), \tag{2}$$

where x^s and y^s are the image and the ground truth annotation, respectively. The first term is the bounding box regression loss and the second term is the classification loss.
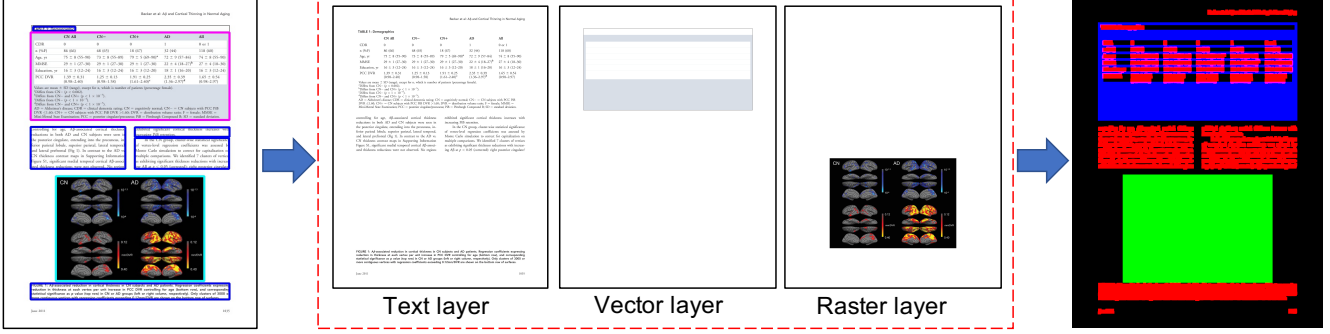
Figure 3. Generating the rendering layer mask from a PDF page. Given a PDF page, we first use a tool to generate the text, raster and vector rendering layers, which are then binarized to separate the foreground from the background. Next, we merge the binary maps of the three layers and get a raw mask. Last, we perform morphological dilation and close operation to fill in the gaps between text characters and the holes in the raster drawings.

4.2. Feature Pyramid Alignment

As we can see above, feature maps in the pyramid are a mixture of both high- and low-level features; aligning feature pyramids from different domains therefore results in a joint alignment of both low- and high-level semantics. This is advantageous over existing methods where alignment is performed for low-level features only [29] or high-level features only [3], or both of them separately [15]. Moreover, by virtue of building upon FPN, we inherit its strength of detecting objects of wide range of sizes, which is important for detecting objects in document images, as they can vary significantly in size. For example, "text" objects can occupy almost a whole page (e.g., long paragraphs), while others may be as small as a few characters or digits (e.g., page numbers or short section headings).

Specifically, FPA includes 4 binary domain classifiers $\{D_1, D_2, D_3, D_4\}$ corresponding to $\{P_1, P_2, P_3, P_4\}$. These classifiers predict the domain labels (source or target) of the pixels in the feature maps. We train the classifiers and FPN in an adversarial manner so that FPN is domain-agnostic once the domain classifiers cannot tell whether a pixel is from the source or target. To this end, we reverse the gradients with respect to $\{P_1, P_2, P_3, P_4\}$ to optimize the min-max problem in each individual back-propagation [6]. The loss function is as follows:

$$\mathcal{L}_p = \quad -\frac{1}{4W^s H^s} \sum_{i=1}^{4} \sum_{w=1}^{W^s} \sum_{h=1}^{H^s} \log(D_i(P_{i,w,h}^s)) - \frac{1}{4W^t H^t} \sum_{i=1}^{4} \sum_{w=1}^{W^t} \sum_{h=1}^{H^t} \log(1 - D_i(P_{i,w,h}^t)),$$

(3)

where W^s, H^s, W^t, and H^t are the width and height of the source and target feature maps, respectively. P_i^s and P_i^t are the i-th layers of the source and target pyramids, respectively.

4.3. Region Alignment

The above FPA module performs pixel-wise dense alignment of the feature maps, which gives equal treatment to the foreground and background regions. However, we are more interested in the foreground regions, as they are more semantically meaningful to the detection task. Region proposals are the likely foreground regions, so we perform further alignment on them.

As shown in [29], a "weak global alignment" of images from different domains results in better cross-domain detection performance, due to the focus on the "hard-to-align" images. The focal loss [22] is introduced to the domain classifier to give less weight to the easy-to-align images in the loss function. Inspired by this, we include focal loss in our region proposal domain classifier to focus more on the hard-to-align proposals. While [29] apply this strategy in image level, we do this at the region proposal level to emphasize the alignment of the foreground regions. It should be noted that while region proposal alignment has been investigated before in [3], it treats all region proposals equally, which could cause the easy-to-align proposals to dominate the loss, leading to undesirable alignment results.

With the introduction of the focal loss, our region alignment objective is as follows:

$$\mathcal{L}_r = \quad -\frac{1}{R} \sum_{i=1}^{R} (1 - D_r(r_i^s))^\gamma \log(D_r(r_i^s)) - \frac{1}{R} \sum_{i=1}^{R} (D_r(r_i^t))^\gamma \log(1 - D_r(r_i^t)),$$

(4)

where R is the number of region proposal extracted; the terms r_i^s and r_i^t are the i-th region proposals extracted from the source and target images, respectively; D_r is the binary domain classifier; and, γ controls the weight on hard-to-align proposals. As in FPA, we reverse the gradients with respect to the proposals and execute adversarial training of the classifier and FPN in each individual back-propagation.

4.4. Rendering Layer Alignment

The PDF pages are rendered into three separate layers, where each layer contains the pixels resulting from a single type of content: text, vector, or raster. These layers provide information about the content within a PDF page. More importantly, they are available and consistent for both source

	text	list	heading	table	figure	MAP
FRCNN (source-only)	61.7	44.9	75.2	72.0	65.4	63.8
SWDA [29]	66.0	23.3	81.0	85.1	71.4	65.3
SWDA+RLA (Ours)	67.4	48.6	82.9	85.3	59.3	**68.7**

Table 1. Impact of adding the proposed RLA module on an existing work. The best results are in **bold**

	text	list	heading	table	figure	MAP
FPN (source-only)	60.9	51.5	74.6	69.6	67.8	64.9
FPN + FPA	68.4	51.9	83.4	68.1	60.5	66.5
FPN + FPA + RA	65.8	52.5	82.3	74.8	67.4	68.6
FPN + FPA + RA + RLA	67.5	53.6	82.1	76.6	73.9	**70.7**

Table 2. Ablation study about the effectiveness of the proposed components. The best results are in **bold**.

and target images. Thus, they can be used as an additional supervision cue to bridge domain gaps. RLA takes advantage of this and utilizes the rendering layers to generate for each page a mask which specifies the drawing type each pixel belongs to. Figure 3 illustrates this process.

The mask can be viewed as a segmentation map for the page images and we can learn a model to predict the map from the image. Therefore, the RLA module is a segmentation neural network which takes feature maps C_4 as input and outputs a dense possibility map of the drawing types of each pixel. The page masks are used as ground truth. Thus, the rendering layer segmentation objective is as follows:

$$\mathcal{L}_s = -\frac{1}{W_m^s H_m^s C} \sum_{i=1}^{W_m^s H_m^s} \sum_{c=1}^{C} y_{i,c} \log p_{i,c}^s - \frac{1}{W_m^t H_m^t C} \sum_{i=1}^{W_m^t H_m^t} \sum_{c=1}^{C} y_{i,c} \log p_{i,c}^t, \quad (5)$$

where W_m^s, H_m^s, W_m^t, and H_m^t are the width and height of the masks for the source and images, respectively; $p_{i,c}^s$ and $p_{i,c}^t$ are the probability of the i-th pixel of being class c; $y_{i,c}$ is the ground truth label; and, C is the the number of classes. We find that the vector drawing class is not reliable, as vector drawings are usually too thin to have a concrete semantic meaning. So, we merge it into the background class and keep "background", "text", and "raster" classes, i.e., $C = 3$.

4.5. Model Training and Inference

The model is trained end-to-end by minimizing the sum of the above losses:

$$\mathcal{L} = \mathcal{L}_{det}^s + \lambda_1 \mathcal{L}_p + \lambda_2 \mathcal{L}_r + \lambda_3 \mathcal{L}_s, \quad (6)$$

where λ_1, λ_2 and λ_3 are three hyper-parameters.

For model inference, we remove the FPA, RA, and RLA modules and keep only the standard FPN. Then, the inference process is the same as the standard detection model: images are fed to the model and the detection bounding boxes are the output.

5. Experiments

Implementation details. As introduced above, we build upon the standard feature pyramid networks (FPN) and propose three novel modules to combat domain shift problem. For FPN, we follow the most common practice and use ResNet-101 as the backbone. There are four domain classifiers in the proposed FPA module; they share the same

structure but not the weights. We adopt the similar structure as [29] and use three convolution layers. The kernel size of the convolution layers is set as one and the padding size is zero. ReLU activation function is applied to the outputs of the first two convolution layers and Sigmoid is used for that of the last one. The RA module consists of three FC layers. ReLU and Dropout are applied on the outputs of the first two FC layers. For the segmentation network in the RLA module, we use the same structure as the DeepLab-V2 [2] and predict the segmentation mask from the feature map.

We train the networks with an SGD optimizer and an initial learning rate of 0.001, which is divided by 10 after every 8 epochs out of the total 12 epochs. For all our experiments, we set $\lambda_1 = \lambda_2 = 0.1$ and $\lambda_3 = 0.01$. Following [29], the focal loss parameter is set as $\gamma = 5.0$.

In all cross-domain experiments, we use the training splits of the source and target datasets for training and evaluate on the test split of the target dataset. During training, only the labels for the source dataset are available. We set the shorter side of the image to 600 pixels. and report mean average precision (MAP) with a threshold of 0.5 to evaluate different methods. We implemented all methods with PyTorch [25].

5.1. Ablation Study

To address the domain shift problem, we propose three novel modules on top of the standard object detection model, namely, feature pyramid alignment (FPA) module, Region Alignment (RA) module, and the Rendering Layer Alignment (RLA) module. To evaluate the effectiveness and impact of the three modules, we conduct an ablation study on the adaption from *Legal* and *PubMed*.

RLA. RLA takes the rendering layers available in both source and target domains as additional alignment cues and trains the network with an auxiliary segmentation task. To evaluate its effectiveness, we first attach it to a recent cross-domain object detection model SWDA [29] and evaluate the resulting performance. The results in Table 1 show that the MAP is boosted by 3.2 points with this module added. Furthermore, as Table 2 shows, when used as a component of our proposed method, RLA raises the MAP from 68.6 to 70.7. These consistent performance gains substantiate RLA's effectiveness.

FPA. FPA performs domain alignment by pushing the feature pyramids of images from different domains closer to-

	Legal → Chn						Chn → Legal					
	text	list	heading	table	figure	MAP	text	list	heading	table	figure	MAP
Oracle	90.5	89.9	90.5	88.9	90.5	90.1	84.5	88.8	82.4	78.6	71.9	81.3
FRCNN (source-only)	73.7	57.9	74.8	66.2	76.5	69.8	60.7	50.9	30.7	47.2	24.1	42.7
FPN (source-only)	75.0	67.3	80.3	65.1	85.2	74.6	59.0	54.5	26.4	53.2	24.7	43.6
SWDA [29]	74.9	67.7	73.8	74.0	86.6	75.4	52.2	51.1	31.9	58.1	29.9	44.6
SWDA + RLA (Proposed)	75.4	73.2	79.1	78.7	87.7	**78.8**	59.2	57.0	33.0	56.0	28.9	46.8
Proposed	76.8	75.5	79.2	72.5	88.2	78.5	62.7	62.3	35.5	57.9	26.9	**49.1**

Table 3. Cross-domain detection results between *Legal* to *Chn*. The "Oracle" results are obtained by FPN trained with labeled training data of the target domain. The best results are in **bold**.

	Chn → PubMed						PubMed → Chn					
	text	list	heading	table	figure	MAP	text	list	heading	table	figure	MAP
Oracle	90.6	68.3	90.3	90.7	90.7	86.1	90.5	89.9	90.5	88.9	90.5	90.1
FRCNN (source-only)	41.3	14.3	45.4	67.4	57.4	45.2	26.6	17.7	19.6	45.5	51.9	32.3
FPN (source-only)	47.2	19.5	47.1	64.3	64.7	48.6	38.4	25.0	26.7	45.9	28.7	32.9
SWDA [29]	56.0	20.3	52.2	81.2	44.5	50.9	53.0	18.5	35.0	64.7	64.3	47.1
SWDA + RLA (Proposed)	50.6	24.3	50.5	74.6	59.2	51.8	48.9	25.3	39.8	60.0	74.3	49.7
Proposed	55.8	28.6	54.1	79.6	52.5	**54.1**	36.7	44.4	42.1	64.3	79.4	**53.4**

Table 4. Cross-domain detection results between *PubMed* to *Chn*.

	Legal → PubMed						PubMed → Legal					
	text	list	heading	table	figure	MAP	text	list	heading	table	figure	MAP
Oracle	90.6	68.3	90.3	90.7	90.7	86.1	84.5	88.8	82.4	78.6	71.9	81.5
FRCNN (source-only)	61.7	44.9	75.2	72.0	65.4	63.8	37.3	37.3	27.1	29.8	8.3	28.0
FPN (source-only)	60.9	51.5	74.6	69.6	67.8	64.9	35.3	41.4	28.5	30.5	3.7	27.8
SWDA [29]	66.0	23.3	81.0	85.1	71.4	65.3	37.3	36.1	44.0	48.5	10.5	35.3
SWDA + RLA (Proposed)	67.4	48.6	82.9	85.3	59.3	68.7	36.8	39.0	43.4	50.7	11.9	**36.4**
Proposed	67.5	53.6	82.1	76.6	73.9	**70.7**	37.1	49.6	42.5	31.1	12.0	34.5

Table 5. Cross-domain detection results between *Legal* and *PubMed*.

gether. Since each layer of the feature pyramids incorporates both low and high features, FPA thus jointly aligns low- and high-level semantics. Table 2 shows that FPA leads to a gain of 1.6 MAP relative to the FPN baseline.

RA. RA enhances the alignment of foreground regions by aligning the extracted region proposals, with a focal loss based learning objective to focus more on the hard-to-align ones. Table 2 shows that it raises MAP from 66.5 to 68.6.

5.2. Comparative Results

We conduct cross-domain evaluation between the three datasets, *Chn*, *Legal* and *PubMed*. The first one is a Chinese document dataset and the latter two are English datasets. We first conduct cross-lingual performance evaluation between *Chn* and *Legal*, and between *Chn* and *PubMed*. Table 3 and Table 4 shows the experimental results. Since *Legal* and *PubMed* belong to different English document categories, there is a domain gap between them. Therefore, we also conduct cross-category detection evaluations between these two datasets. Table 5 shows the results.

We observe similar behavior across the three tables. The FPN baseline usually outperforms the FRCNN baseline. This is because document objects vary significantly in size, which FPN is more able to deal with. SWDA builds on top

of FRCNN, leading to consistent performance gains. This shows that some domain adaptation techniques are applicable for various image types. Adding the document-specific alignment module RLA to SWDA results in consistent performance gains for all cases. This substantiates the ability of RLA to mitigate the domain shift problem. Our proposed method builds upon FPN and introduces three novel components. The tables demonstrate that it significantly outperforms the FPN baseline and also SWDA for almost all the cases. In addition, with the RLA module, our method surpasses SWDA for almost all experiments. This suggests that our proposed FPA and RA modules are superior to their counterparts in SWDA. Despite these improvements, the results are still far lower than the oracle setting in which FPN is trained on labeled data from the target domains. This shows that domain shifts are indeed a serious problem for DOD and they have not been fully addressed.

One may have noticed from Table 4 that there is a huge performance jump for SWDA over the FRCNN baseline when adapting *PubMed* to *Chn*: MAP is improved from 32.3 to 47.1. Similarly, in Table 5, SWDA raises MAP over the FRCNN baseline from 28.0 to 35.3 when adapting *PubMed* to *Legal*. We believe the reason for such huge gains is that *PubMed* is comprised of page images of scien-
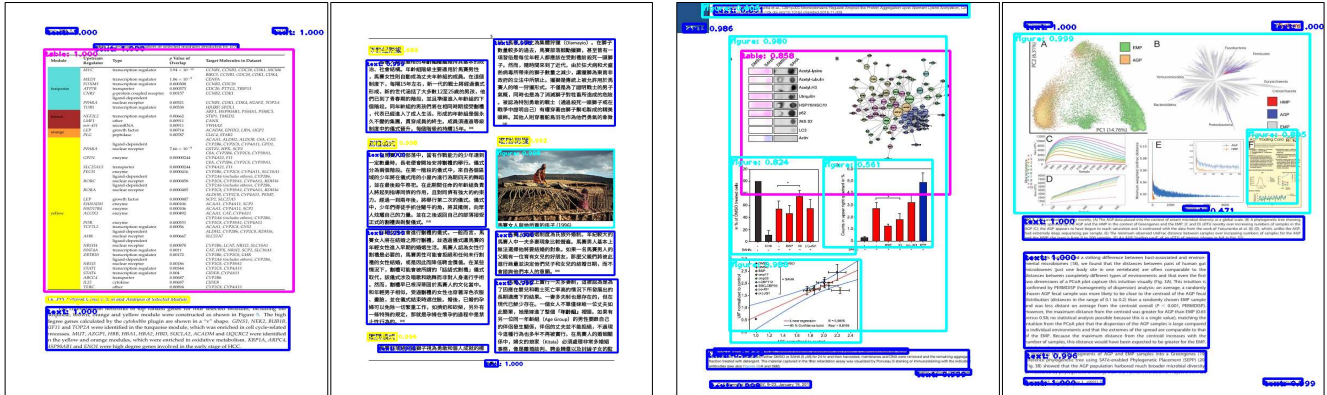
Figure 4. Sample detection results.

	$Kitti \rightarrow Cityscape$	$Cityscape \rightarrow Kitti$
SWDA [29]	41.8	70.6
Proposed	42.9	73.3

Table 6. Cross-domain detection results for natural scene images.

tific journal articles that share similar formatting templates. So, the diversity of this dataset is limited. A model trained with labeled data of this dataset should be able to effectively handle other data within the dataset, as evidenced by the high oracle results, but it is less likely to generalize to other datasets. This problem is not as severe for the other two datasets, *Chn* and *Legal*, because the diversity is carefully considered when synthesizing *Chn* and selecting data of *Legal* for annotation. So, the impact of domain adaption is much more significant for *PubMed* than the other two datasets when they are used as the source domain.

5.3. Further Analysis

Experiments on natural images. Without the proposed RLA module, which is specially designed for the DOD task, our method (FPN plus the FPA and RA modules) can be applied on natural scene images as well. Following the previous methods [3, 15], we conduct cross-domain "car" detection evaluation on the *Cityscape* [4] and *Kitti* [10] datasets. There are 14999 images in the *Kitti* dataset and we chose 7481 images in the training set for both adaptation and evaluation. The *Cityscape* dataset has 3475 images and we use 2975 images for adaptation training and the remaining 500 images for evaluation. The results in Table 6 show that our method also outperforms SDWA for the natural scene image cross-domain detection task, especially for adaptation from *Cityscape* and *Kitti*, where we achieve 2.7% improvement for the AP of car. This set of experiment further substantiates the efficacy of the proposed adaptation modules.

Visualization of detection results. Figure 4 visualizes some detection results from *Chn* and *PubMed*. We can see that the proposed method in most cases can successfully decompose a complex page into semantically meaningful re-

gions, with high localization precision and confident classification scores for objects of extremely diverse sizes. For example, in the first image, both the large table which covers about two-third of the page and the tiny pagination are perfectly detected. However, the proposed method tends to make mistakes for ambiguous objects whose semantic meanings can be correctly determined only within the context. For example, in the fourth (right-most) image, there is a composite figure comprised of six sub-figures. Each sub-figure alone is a figure instance. But when considering the context, it is wrong to detect them as object instances individually. Similar cases also appear in the third image.

6. Conclusion

We investigate cross-domain document object detection by proposing a benchmark suite and a novel method. The benchmark suite includes different types of datasets on which cross-domain document object detectors can be trained and evaluated. For each dataset, we provide not only the essential components, page images and bounding boxes annotations, but also auxiliary components, raw PDF files and the PDF rendering layers. The proposed model builds upon the standard object detection model with three novel domain alignment modules, namely, the feature pyramid alignment (FPA) module, the Region Alignment (RA) module, and Rendering Layer Alignment (RLA) module. Experiments on the benchmark suite confirm the effectiveness of the proposed novel components and that the proposed method significantly outperforms the baseline methods. In addition, the proposed method also improves over the state-of-the-art method for cross-domain object detection on natural scene images.

References

[1] Roldano Cattoni, Tarcisio Coianiz, Stefano Messelodi, and Carla Maria Modena. Geometric layout analysis techniques for document image understanding: a review. *ITC-irst Technical Report*, 9703(09), 1998.

[2] Liang-Chieh Chen, George Papandreou, Iasonas Kokkinos, Kevin Murphy, and Alan L Yuille. Deeplab: Semantic image segmentation with deep convolutional nets, atrous convolution, and fully connected crfs. *IEEE Transactions on Pattern Analysis and Machine Intelligence*, 40(4):834–848, 2017.

[3] Yuhua Chen, Wen Li, Christos Sakaridis, Dengxin Dai, and Luc Van Gool. Domain adaptive faster r-cnn for object detection in the wild. In *CVPR*, 2018.

[4] Marius Cordts, Mohamed Omran, Sebastian Ramos, Timo Rehfeld, Markus Enzweiler, Rodrigo Benenson, Uwe Franke, Stefan Roth, and Bernt Schiele. The cityscapes dataset for semantic urban scene understanding. In *CVPR*, 2016.

[5] Jing Fang, Xin Tao, Zhi Tang, Ruiheng Qiu, and Ying Liu. Dataset, ground-truth and performance metrics for table detection evaluation. In *DAS*, 2012.

[6] Yaroslav Ganin and Victor Lempitsky. Unsupervised domain adaptation by backpropagation. In *ICML*, 2015.

[7] Liangcai Gao, Xiaohan Yi, Zhuoren Jiang, Leipeng Hao, and Zhi Tang. Icdar2017 competition on page object detection. In *ICDAR*, 2017.

[8] Liangcai Gao, Xiaohan Yi, Yuan Liao, Zhuoren Jiang, Zuoyu Yan, and Zhi Tang. A deep learning-based formula detection method for pdf documents. In *ICDAR*, 2017.

[9] Utpal Garain. Identification of mathematical expressions in document images. In *ICDAR*, 2009.

[10] Andreas Geiger, Philip Lenz, Christoph Stiller, and Raquel Urtasun. Vision meets robotics: The kitti dataset. *The International Journal of Robotics Research*, 32(11):1231–1237, 2013.

[11] Azka Gilani, Shah Rukh Qasim, Imran Malik, and Faisal Shafait. Table detection using deep learning. In *ICDAR*, 2017.

[12] Max Göbel, Tamir Hassan, Ermelinda Oro, and Giorgio Orsi. Icdar 2013 table competition. In *ICDAR*, 2013.

[13] Dafang He, Scott Cohen, Brian Price, Daniel Kifer, and C Lee Giles. Multi-scale multi-task fcn for semantic page segmentation and table detection. In *ICDAR*, 2017.

[14] Kaiming He, Xiangyu Zhang, Shaoqing Ren, and Jian Sun. Deep residual learning for image recognition. In *CVPR*, 2016.

[15] Zhenwei He and Lei Zhang. Multi-adversarial faster-rcnn for unrestricted object detection. In *ICCV*, 2019.

[16] Naoto Inoue, Ryosuke Furuta, Toshihiko Yamasaki, and Kiyoharu Aizawa. Cross-domain weakly-supervised object detection through progressive domain adaptation. In *CVPR*, 2018.

[17] Mehran Khodabandeh, Arash Vahdat, Mani Ranjbar, and William G Macready. A robust learning approach to domain adaptive object detection. In *ICCV*, 2019.

[18] Seunghyeon Kim, Jaehoon Choi, Taekyung Kim, and Changick Kim. Self-training and adversarial background regularization for unsupervised domain adaptive one-stage object detection. In *ICCV*, 2019.

[19] Taekyung Kim, Minki Jeong, Seunghyeon Kim, Seokeon Choi, and Changick Kim. Diversify and match: A domain adaptive representation learning paradigm for object detection. In *CVPR*, 2019.

[20] Xiao-Hui Li, Fei Yin, and Cheng-Lin Liu. Page object detection from pdf document images by deep structured prediction and supervised clustering. In *ICPR*, 2018.

[21] Tsung-Yi Lin, Piotr Dollár, Ross Girshick, Kaiming He, Bharath Hariharan, and Serge Belongie. Feature pyramid networks for object detection. In *CVPR*, 2017.

[22] Tsung-Yi Lin, Priya Goyal, Ross Girshick, Kaiming He, and Piotr Dollár. Focal loss for dense object detection. In *ICCV*, 2017.

[23] Xiaoyan Lin, Liangcai Gao, Zhi Tang, Xiaofan Lin, and Xuan Hu. Mathematical formula identification in pdf documents. In *ICDAR*, 2011.

[24] Ning Liu, Dongxiang Zhang, Xing Xu, Long Guo, Lijiang Chen, Wenju Liu, and Dengfeng Ke. Robust math formula recognition in degraded chinese document images. In *ICDAR*, 2017.

[25] Adam Paszke, Sam Gross, Soumith Chintala, Gregory Chanan, Edward Yang, Zachary DeVito, Zeming Lin, Alban Desmaison, Luca Antiga, and Adam Lerer. Automatic differentiation in pytorch. 2017.

[26] Deepak Pathak, Philipp Krahenbuhl, Jeff Donahue, Trevor Darrell, and Alexei A Efros. Context encoders: Feature learning by inpainting. In *CVPR*, 2016.

[27] Shaoqing Ren, Kaiming He, Ross Girshick, and Jian Sun. Faster r-cnn: Towards real-time object detection with region proposal networks. In *NuerIPS*, 2015.

[28] Aruni RoyChowdhury, Prithvijit Chakrabarty, Ashish Singh, SouYoung Jin, Huaizu Jiang, Liangliang Cao, and Erik Learned-Miller. Automatic adaptation of object detectors to new domains using self-training. In *CVPR*, 2019.

[29] Kuniaki Saito, Yoshitaka Ushiku, Tatsuya Harada, and Kate Saenko. Strong-weak distribution alignment for adaptive object detection. In *CVPR*, 2019.

[30] Sebastian Schreiber, Stefan Agne, Ivo Wolf, Andreas Dengel, and Sheraz Ahmed. Deepdesrt: Deep learning for detection and structure recognition of tables in document images. In *ICDAR*, 2017.

[31] Peter WJ Staar, Michele Dolfi, Christoph Auer, and Costas Bekas. Corpus conversion service: A machine learning platform to ingest documents at scale. In *KDD*, 2018.

[32] Dieu Ni Tran, Tuan Anh Tran, Aran Oh, Soo Hyung Kim, and In Seop Na. Table detection from document image using vertical arrangement of text blocks. *International Journal of Contents*, 11(4):77–85, 2015.

[33] Xiao Yang, Ersin Yumer, Paul Asente, Mike Kraley, Daniel Kifer, and C Lee Giles. Learning to extract semantic structure from documents using multimodal fully convolutional neural networks. In *CVPR*, 2017.

[34] Xiaohan Yi, Liangcai Gao, Yuan Liao, Xiaode Zhang, Run-tao Liu, and Zhuoren Jiang. Cnn based page object detection in document images. In *ICDAR*, 2017.

[35] Xu Zhong, Jianbin Tang, and Antonio Jimeno Yepes. Pub-laynet: largest dataset ever for document layout analysis. *arXiv preprint arXiv:1908.07836*, 2019.

[36] Jun-Yan Zhu, Taesung Park, Phillip Isola, and Alexei A Efros. Unpaired image-to-image translation using cycle-consistent adversarial networks. In *ICCV*, 2017.

[37] Xinge Zhu, Jiangmiao Pang, Ceyuan Yang, Jianping Shi, and Dahua Lin. Adapting object detectors via selective cross-domain alignment. In *CVPR*, 2019.